Poly(ethene-*co*-norbornene) Obtained with a Constrained Geometry Catalyst. A Study of Reaction Kinetics and Copolymer Properties

Knut Thorshaug, Raniero Mendichi, Laura Boggioni, and Incoronata Tritto*

Istituto di Chimica delle Macromolecole del C.N.R., via E. Bassini 15, I-20133 Milano, Italy

Stefan Trinkle, Christian Friedrich, and Rolf Mülhaupt

Freiburger Materialforschungszentrum und Institut für Makromolekulare Chemie der Albert-Ludwigs-Universität, Stefan-Meier-Strasse 21, D-79104 Freiburg i. Br., Germany

Received November 8, 2001; Revised Manuscript Received January 29, 2002

ABSTRACT: Poly(ethene-*co*-norbornene) was synthesized in toluene using $Me_2Si(Me_4Cp)(N^tBu)TiCl_2$ activated with methylaluminoxane (MAO) as catalyst. We found that at 50 °C the molecular weight increases with time for up to 1 h, and very little chain transfer occurs; thus, the copolymerization can be considered as quasi-living. The quasi-living nature requires high norbornene feed fractions; it is more pronounced at low temperatures and short reaction times. $M_w/M_n = 1.3$ ($M_n = 100$ kg/mol) was the lowest polydispersity index obtained when the copolymerization reaction was conducted at 50 °C. Poly(ethene-*co*-norbornene) containing long chain branches was obtained; the degree of branching decreased with an increasing norbornene molar fraction in the feed. The presence of long chain branches was confirmed by both size exclusion chromatography and rheology; the branches were found evenly distributed in the copolymers. Rheology of poly(ethene-*co*-norbornene) was analyzed; the $G_N°$ minimum could be reached, most probably, because bulky bicyclic norbornene units inhibit crystallization. Compared to the literature data, the low level of long chain branches incorporated into our poly(ethene-*co*-norbornene) samples does not significantly affect the glass transition temperature. The relationship between the experimental conditions and the polymer architecture is discussed on the basis of the proposed reaction scheme.

1. Introduction

Copolymers of ethene and norbornene (poly(E-*co*-N)) obtained with single-site catalysts are amorphous materials with an interesting combination of a high glass transition temperature (T_g), transparency, and a heat resistance.[1,2] Following the discovery of methylaluminoxane (MAO),[3] several single-site catalysts have been developed,[4−6] some of which have also been used for the poly(E-*co*-N) synthesis. The constrained geometry catalysts (CGC)[7,8] have an open structure, and their metal center may easily be accessed by bulky monomers such as norbornene. Among several CGC complexes, $Me_2Si(Me_4Cp)(N^tBu)TiCl_2$ (**1**) (Scheme 1) shows the highest catalytic activity in ethene−norbornene copolymerization reactions when activated with MAO;[9−11] the copolymers contain both *meso* and *racemic* alternating E−N-sequences as well as isolated norbornene units.[12]

CGC-based catalytic systems have a unique ability to incorporate long chain branches (LCB) in the polymers when used in ethene homopolymerization, with 0.01−3 LCB/1000C atoms claimed as typical values.[13] It has been suggested that, in the case of **1**/MAO, the LCB formation occurs by β-H transfer to the monomer followed by reinsertion of the macromonomer.[14,15] Until now, it has not been clarified to what extent **1**/MAO is able to incorporate LCB into poly(E-*co*-N). In addition to LCB incorporation, short chain branches (SCB) can be incorporated into polyethene using **1**/MAO as a catalyst along with a higher α-olefin, e.g., 1-eicosene.[16] The presence of LCB and/or SCB can be expected to influence properties of the poly(E-*co*-N), e.g., can improve its processability.

Scheme 1. $Me_2Si(Me_4Cp)(N^tBu)TiCl_2$ (1)

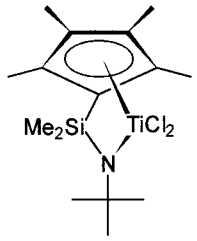

(**1**)

Recently, some of us reported the quasi-living character of ethene−norbornene copolymerization using *ansa*-zirconocenes.[17] Quasi-living polymerization implies a growth of the molecular weight with reaction time *and* occurrence of chain-transfer reactions. Although not ideally living, the quasi-living nature offers a route to an improved control of the molar mass distribution (MMD) compared to nonliving systems. Motivated by the possibility of obtaining poly(E-*co*-N) with both a controlled LCB frequency and MMD, we initiated a study of ethene−norbornene copolymerization using **1**/MAO as a catalyst. Some characteristics of this system have been reported earlier,[9,11,12] but there are several aspects that deserve more attention. Herein, using **1**/MAO as a catalyst for ethene−norbornene copolymerization, we report on the reaction kinetics, the quasi-living nature of the copolymerization reaction, and the possibility of incorporating LCB in poly(E-*co*-N). We use size-exclusion chromatography (SEC) and rheology to characterize the copolymers, with emphasis on LCB analysis. Finally, we studied the influence of LCB on thermal properties of the copolymers.

* Corresponding author: e-mail: tritto@icm.mi.cnr.it.

10.1021/ma011949o CCC: $22.00
Published on Web 03/15/2002

2. Establishing a Sound SEC Method for Characterization of Long Chain Branches in Poly(ethene-*co*-norbornene)

SEC, and in particular, branching analysis, of a copolymer is not a simple matter. We, therefore, verified the soundness of the chosen approach before applying it to our poly(E-*co*-N) samples. In principle, LCB can be quantified by several methods, such as NMR,[14,18,19] rheology,[20] and SEC, using on-line light scattering or viscometer detectors.[21,22] In the case of poly(E-*co*-N), LCB detection by NMR is severely hampered by complexity of the spectra, and an assignment of signals in poly(E-*co*-N) related to LCB is not readily available. It is not justified to assume that the ^{13}C NMR shift values used for LCB detection in polyethene to be valid for poly(E-*co*-N) as well, since such values depend on the (unknown) distance between the branch point and the bicyclic units in the copolymer. We therefore opted for LCB characterization by SEC with on-line viscometry. To firmly establish SEC as a reliable method, selected samples where also analyzed *by rheology*. In all samples analyzed by both SEC and rheology, rheology confirmed the conclusion concerning the polymer architecture, i.e., whether LCB were present or not.

Using a SEC system with an on-line viscometer, the starting point in the LCB analysis is the $[\eta] = f(M)$ power law, the Mark−Houwink−Sakurada (MHS) plot. The SEC−DV system provides instantaneous values of the molar mass M_i and the intrinsic viscosity $[\eta]_i$ at each elution volume. Hence, in the case of a sample with a broad molar mass distribution (MMD), one obtains the MHS plot in a single SEC run. The utmost care must be taken when analyzing copolymers since the signal of the concentration detector (DRI) depends on the copolymer composition. In short, the instantaneous polymer concentration c_i is essential in the estimation of $[\eta]_i$, and the MHS plot of a copolymer, from which one estimates the degree of branching, is sensitive to any shift in the chemical composition. In the present work (section 3.1), sampling from the reaction mixture demonstrated that the chemical composition of our poly(E-*co*-N) samples does not depend on the chain length (reaction time). Thus, we can assume that the chemical composition of each poly(E-*co*-N) sample is constant for any chain length. In this case, the DRI detector can be considered a true concentration detector. In addition, to demonstrate that the curvature of the MHS plot of our poly(E-*co*-N) samples is not an artifact due to any possible chemical composition drift, a selected number of linear and branched poly(E-*co*-N) samples were also characterized *by rheology*. Again, rheology confirmed the presence of LCB in all branched poly(E-*co*-N) samples (see section 3.3). Thus, the chosen approach to detect LCB by SEC−DV is reliable.

Having established a sound method in order to *qualitatively* detect LCB in poly(E-*co*-N) by SEC−DV, we now turn to *quantitative* estimates of the LCB frequency in the copolymers. Estimation of LCB frequency has been achieved by several authors,[23,24] but the estimated values depend on the method used in the characterization and a priori assumptions. LCB analysis starts from the definition of the branching index g[25] or the correlated g' index. The branching index g is defined as the ratio between $\langle s^2 \rangle$ for branched and linear macromolecules identical in the molar mass, where $\langle s^2 \rangle$ is the mean-square radius (size) of the macromolecules. Because it is simpler to measure $[\eta]$ rather than $\langle s^2 \rangle$, a second branching index, g', was introduced[22] and defined as the ratio between $[\eta]$ of branched and linear macromolecules with identical molar masses: $g' = 1$ for a linear polymer and $g' < 1$ in the presence of branches. Relevant relationships are reported in eqs 1−3, assuming trifunctional branching points, the assumption which we used in the present LCB analysis.

$$g = \frac{\langle s^2 \rangle_b}{\langle s^2 \rangle_l} \tag{1a}$$

$$g' = \frac{[\eta]_b}{[\eta]_l} \tag{1b}$$

$$g' = g^{\epsilon} \tag{1c}$$

$$M_b = M_l \tag{1d}$$

$$g = g'^{1/\epsilon} = \left[\left(1 + \frac{B_n}{6}\right)^{1/2} + \frac{4B_n}{9\pi}\right]^{-1/2} \tag{2}$$

$$\lambda_n = \frac{B_n}{M_n} \tag{3a}$$

$$\mathrm{LCB}_{1000C} = \lambda_n M_{1000C} \tag{3b}$$

where B_n is the number of branches per macromolecule, λ_n is the LCB frequency per unit of molar mass, LCB_{1000C} is the LCB frequency per 1000 carbon atoms, M_{1000C} is the molar mass of a polymer chain containing 1000 carbon atoms, and the subscripts b, l, n are used to denote branched, linear, and numeric-average values, respectively. We have assumed the form factor ϵ to be 1.2,[23] supposing random branching. Obviously, $M_{1000C} = 14\,000$ for polyethene, and in the case of poly(E-*co*-N), we introduce a correction for the presence of norbornene units by using the relationship $M_{1000C} = (^1/_2 \times 94 \times w_N + ^1/_2 \times 28 \times (1 - w_N)) \times 1000$, where w_N denotes the weight fraction of norbornene in a copolymer.

3. Results and Discussion

In the first section, we address the reaction kinetics, and in the second and the third parts we focus on polymer characterization by SEC and rheology. The final part is devoted to the thermal properties of the copolymers. We present a reaction scheme (Scheme 2) which can be used to rationalize observations presented in the first three parts. Tables describing the reaction conditions and characteristics of each sample are given as Supporting Information.

3.1. Reaction Kinetics. Copolymerization propagation kinetics can be described by Markov statistics, with first- and second-order models being most frequently used. We measured the average molar fractions of norbornene in the copolymers ($x_{N,copolymer}$) by both ^{13}C NMR[26] and GPC[27] and fitted[28] the copolymerization equations for first- and second-order Markov statistics[29] to the experimental data.[30] The obtained reactivity ratios are given in Table 1. Details of the copolymer microstructure are beyond the scope of this work[12d] and were not utilized in the calculations of the reactivity ratios. The reactivity values agree with the reports[9a,11,12] that poly(E-*co*-N) obtained with **1**/MAO is mainly al-

Scheme 2. Reaction Paths Proposed To Take Part in the Catalytic Cycle during Ethene−Norbornene Copolymerization Catalyzed by 1/MAO[a]

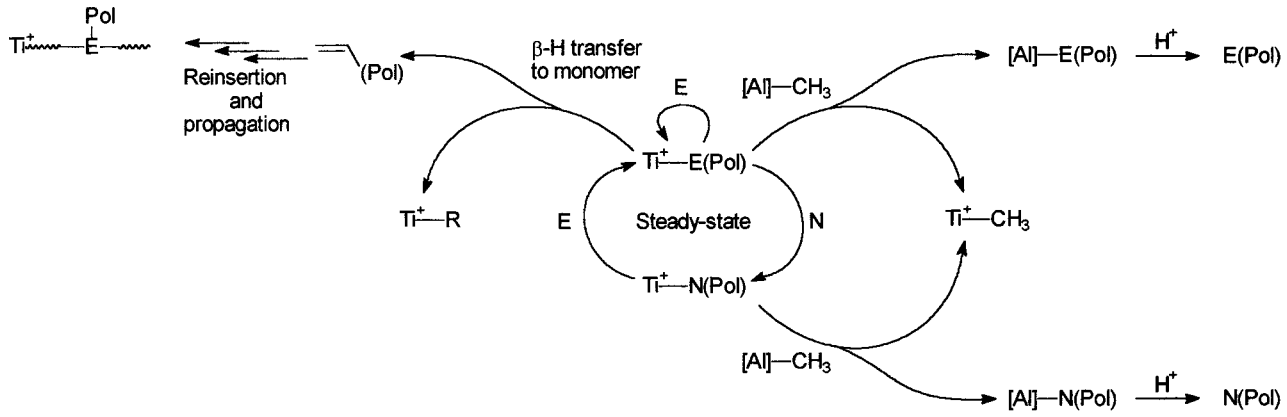

[a] Center: propagation. Upper left: LCB formation. Upper right: chain transfer to Al from an E*-site. Lower right: chain transfer to Al from an N*-site. The $Ti^{+}-R$ cations may take further part in the catalytic cycle. For all species, the ligands, counterions, and solvent have been omitted for clarity.[38]

Table 1. Ethene−Norbornene Reactivity Ratios Calculated from the Overall Composition Data Using First- and Second-Order Markov Statistics. Conditions: 1/MAO in Toluene, T_{rx} = 50 °C, p_{ethene} = 1.1 atm, 0 < $x_{N,feed}$ < 0.983, 0 < $x_{N,copolymer}$ < 0.456, Maximum Norbornene Conversion = 7.6%

	first-order Markov			second-order Markov				
	r_1	r_2	residual[a]	r_{11}	r_{12}	r_{21}	r_{22}	residual[a]
SEC	3.3	0.0	1.7×10^{-2}	3.0	0.0	7.0	0.0	1.3×10^{-2}
^{13}C NMR	3.8	0.0	4.1×10^{-3}	2.9	0.0	7.3	0.0	1.8×10^{-3}

[a] Calculated as residual = $[\sum(x_{N,copolymer} - x_{N,calc})^2]/(n - v)$, where $x_{N,copolymer}$ is the experimentally determined norbornene molar fraction in the copolymers, $x_{N,calc}$ is the theoretical norbornene molar fraction in the copolymer calculated from either the first or second Markov model, n is the number of experimental data points in the series (n = 10), and v is the number of parameters in the Markov model (first order, v = 2; second order, v = 4).

ternating ($r_1 r_2 \ll 1$), the norbornene diad fraction is very low, and there are no norbornene triads or longer blocks ($r_2 \approx 0$).

Based on the overall composition data, the second-order model gives a slightly better fit than the first order, but the difference between the two models is insignificant. The first-order Markov model is therefore applied in the following discussion. Sites containing norbornene (N*-site) and ethene (E*-site) as ultimate monomer units are the two different active species. Although this is a simple model, it is sufficient to rationalize observations reported below.

Figures 1−3 summarize our findings concerning the changes of the copolymer yield and of MMD with reaction time, as studied by sampling the reaction mixture at fixed-time intervals.[17] This procedure allows us to investigate the polymer yield and polymer properties as a function of reaction time in a single run. Figure 1 shows that the polymer concentration in the reaction vessel increased linearly with time at 30 and 50 °C whereas at 70 °C *a curvature is observed*. Increasing the feed fraction of norbornene ($x_{N,feed}$) at 50 °C resulted in a decrease of the polymer production rate although a linear time dependence was still observed, as shown in Figure 2. No induction period could be observed; thus, the catalyst activation occurs rapidly at all temperatures and at all norbornene feed fractions. The copolymer composition in each sample was determined by SEC;[27] it remained constant with reaction time.

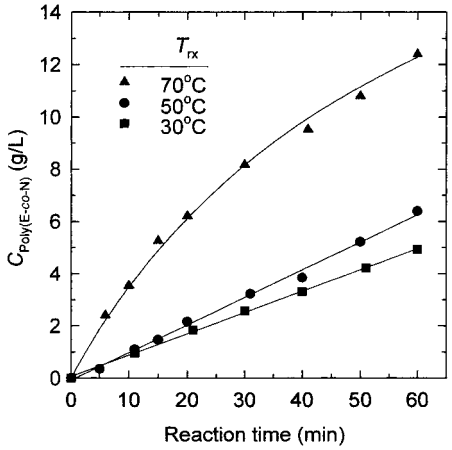

Figure 1. Copolymer concentration ($C_{Poly(E-co-N)}$) in the reactor as a function of reaction time at different reaction temperatures (T_{rx}) with fixed $x_{N,feed}$ = 0.956. Norbornene conversion after 60 min of reaction = 1.0% (30 °C), 1.7% (50 °C), and 4.3% (70 °C).

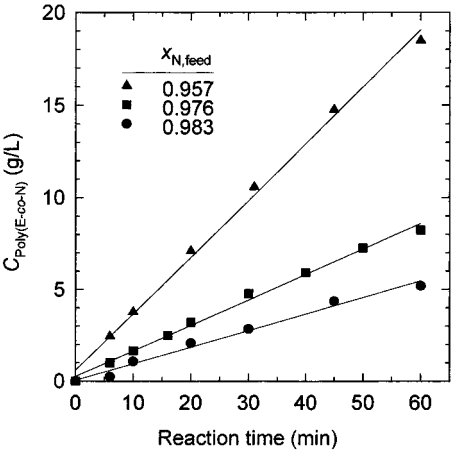

Figure 2. Copolymer concentration ($C_{Poly(E-co-N)}$) in the reactor as a function of reaction time at different norbornene feed fractions ($x_{N,feed}$). Reaction temperature = 50 °C; norbornene conversion after 60 min of reaction = 6.6% ($x_{N,feed}$ = 0.957), 1.6% ($x_{N,feed}$ = 0.976), and 0.72% ($x_{N,feed}$ = 0.983).

The observed rate of polyolefin formation using single-site catalysts can be described by summarizing the rates of several elementary reactions.[3c,31−33] Since the curves

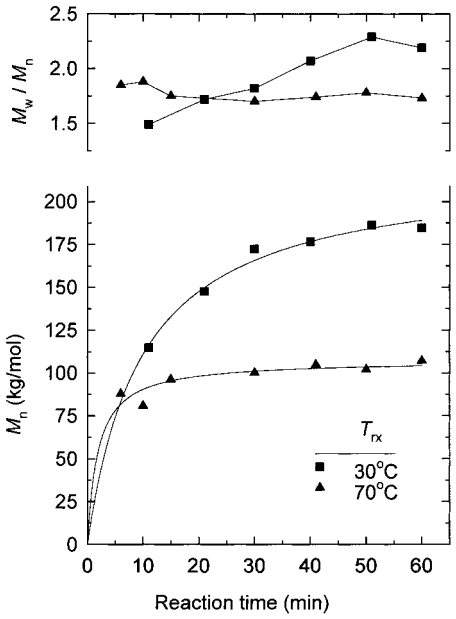

Figure 3. Upper: polydispersity index (M_w/M_n). Lower: number-average molar mass (M_n) as a function of reaction time and reaction temperature (T_{rx}) at fixed $x_{N,feed}$ = 0.956. Norbornene conversion after 60 min of reaction = 1.0% (30 °C) and 4.3% (70 °C).

in Figures 1 and 2 are linear for the reactions conducted at 30 and 50 °C, the steady state between the E*-sites and N*-sites is quickly established and maintained throughout the polymerization reactions without formation of permanently deactivated sites. All plots in Figure 2 are linear; thus, changing $x_{N,feed}$ in the studied range does not affect catalyst stability at 50 °C. The curvature observed for the polymerizations conducted at 70 °C (Figure 1) may be interpreted as a consequence of permanent deactivation. The lower activity with increasing $x_{N,feed}$ reported in Figure 2 can be explained by an increase in the concentration of N*-sites at the expense of E*-sites. It seems reasonable that propagation is slower at N*-sites than E*-sites due to a higher steric hindrance in the former. We assume the number of active sites is the same in all runs since they were all performed at the same [Al]/[Ti] ratio.

Figure 3 shows that, at low reaction temperatures and high $x_{N,feed}$, norbornene decreases both the propagation and the termination rates to such a degree that the growth of the number-average molecular weights (M_n) and polydispersity indexes (M_w/M_n) are observable at reaction times for up to 1 h. A growth of M_n in time is characteristic for living polymerization, but under the given conditions, a deviation of the experimental M_n values from the theoretical ones shows that chain transfer does occur.[34] This is further illustrated in Figure 4. Thus, ethene−norbornene copolymerization catalyzed by **1**/MAO is quasi-living, and it occurs only at high $x_{N,feed}$. By decreasing the reaction temperature from 70 to 30 °C (at constant $x_{N,feed}$ = 0.956), the quasi-living effect was enhanced, as shown in Figure 3. By keeping the reaction temperature constant, at 50 °C, and increasing $x_{N,feed}$ to 0.983, a quasi-living behavior was still observed, and a copolymer with M_n = 100 kg/mol and M_w/M_n = 1.3 was obtained after a 10 min reaction with a very low yield (4.9 mg in 20 mL volume). These were the lowest M_n and M_w/M_n values found in our study. Some of us recently reported on the quasi-living behavior of ethene−norbornene copolymerization

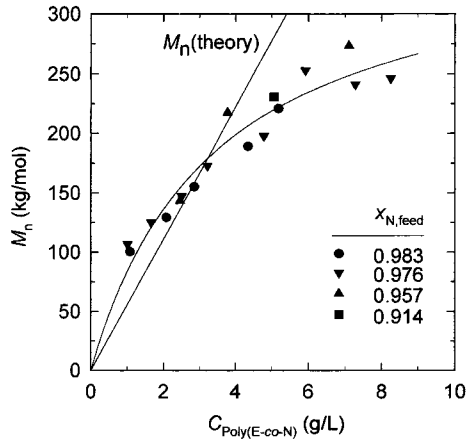

Figure 4. Theoretical and experimental M_n values at different norbornene feed fractions ($x_{N,feed}$). Reaction temperature: 50 °C. Norbornene conversion/reaction time ($x_{N,feed}$) = 3.7%/6 min (0.914), 1.3%/20 min (0.957), 1.6%/60 min (0.976), and 0.72%/60 min (0.983).

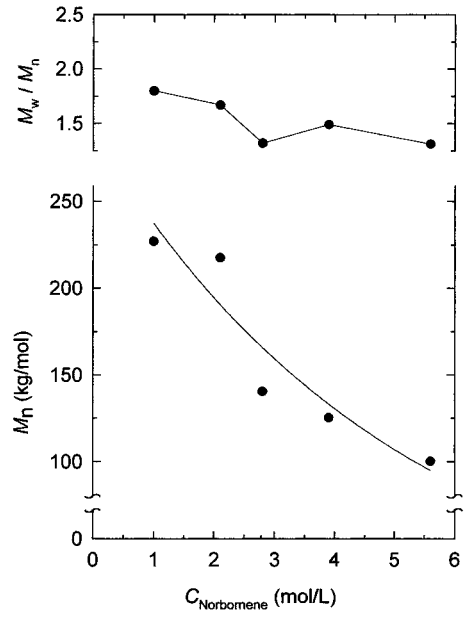

Figure 5. Upper: polydispersity index (M_w/M_n). Lower: number-average molar mass (M_n) as a function of norbornene feed concentration ($C_{Norbornene}$) after 10 min of reaction. Reaction temperature = 50 °C; norbornene conversion ($C_{Norbornene}$) = 8.3% (1.0 mol/L), 1.3% (2.1 mol/L), 0.3% (2.8 mol/L), 0.3% (3.9 mol/L), and 0.2% (5.6 mol/L).

using *ansa*-zirconocenes,[17] but to the best of our knowledge, it has never before been reported for CGC precursors.

At $x_{N,feed}$ = 0.838 and 50 °C, we did not observe any growth of M_n with time, and M_w/M_n was close to 2.0 when sampled after 6 min and afterward. The observation that M_n and M_w/M_n growth with time requires high $x_{N,feed}$ is further illustrated in Figure 5. After 10 min, a decrease in both M_n and M_w/M_n was observed with increasing $x_{N,feed}$. A decrease in the molecular weight with increasing norbornene feed fraction has earlier been reported for **1**/MAO,[9d] using somewhat different experimental conditions than those used in the present work, but an explanation of the observation was not given. The quasi-living nature of the copolymerization, reported for the first time here for **1**/MAO, seems highly relevant. We propose that a slower chain growth with increasing $x_{N,feed}$ explains, at least partly, the decrease

Table 2. Kinetic Parameters for Ethene−Norbornene Copolymerization in Toluene Using 1/MAO

T_{rx}[a] (°C)	x_{Ti*}[b]	$\langle f_p \rangle$[c] (1/s)	$\langle f_t \rangle$[d] (1/s)	$M_n(\infty)$[e] (kg/mol)
30	0.22	6.3	0.10	220
70	0.48	18	0.62	113

[a] Reaction temperature. [b] Fraction of active Ti centers. [c] Average propagation turnover frequency. [d] Average termination turnover frequency. [e] Number-average molar mass at infinite reaction time.

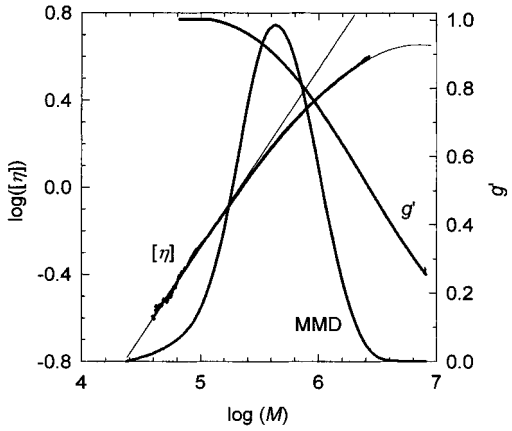

Figure 6. Molecular weight distribution (MMD), Mark−Houwink−Sakurada plot ([η]), and the branching index (g') as a function of log(M) for poly(E-*co*-N) with $x_{N,copolymer} = 0.44$.

in M_n with increasing norbornene feed concentration observed at short reaction times.

The quasi-living character of the copolymerization reaction can be used in order to get quantitative estimates of the fraction of active sites and turnover frequencies. In Table 2, we list the kinetic parameters found by analyzing the data presented in Figures 1−4 according to standard equations for living polymerization.[35−37] The present analysis does not allow for a discrimination between E*-sites and N*-sites; thus, only observable average values are reported. However, it is interesting to note that both the average propagation and termination frequencies, along with the concentration of active Ti centers, increase when the reaction temperature is increased from 30 to 70 °C. The average propagation frequency increase by a factor of almost 3, whereas the average termination frequency increases approximately by a factor of 6. This is consistent with the observed lowering of the number-average molecular weight reached after infinite reaction time by increasing the reaction temperature from 30 to 70 °C. The fraction of active sites found in the present study is significantly lower than those reported for ethene−norbornene copolymerization using *ansa*-metallocenes.[37]

3.2. Long Chain Branches Detected by SEC. It is well-known that polyethene synthesized using **1**/MAO as catalyst contains LCB,[13] whereas this has not yet been studied for poly(E-*co*-N). Since LCB greatly influences the final polymer properties, a qualitative and quantitative characterization of the degree of branching is important. Having established SEC as a reliable method for the LCB detection and quantification in our poly(E-*co*-N) samples, as outlined in the details above, we applied it to characterize LCB in our poly(E-*co*-N) samples.

Figure 6 shows the MHS plot of a branched poly(E-*co*-N) sample, along with the MMD of the copolymer, the linear part of the MHS plot, and the $g' = f$(M) plot

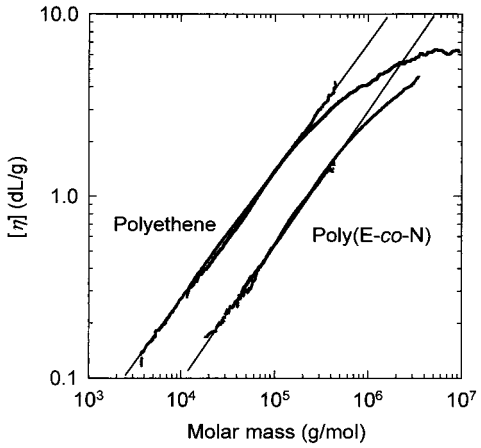

Figure 7. Comparison of the Mark−Houwink−Sakurada plot for linear and long chain branched polyethene and poly(E-*co*-N) with $x_{N,copolymer} = 0.40$ (linear) and $x_{N,copolymer} = 0.44$ (long chain branched), respectively.

calculated from eqs 1−3. One can clearly detect branches in the copolymers by looking at either the curved [η] vs log(M) plot or the drop in g' from 1.0 to 0.25 with increasing log(M).

In Figure 7, we compare the MHS plot of linear and branched polyethene along with linear and branched poly(E-*co*-N). The linear polyethene was the NBS1475 standard, and the linear poly(E-*co*-N) was synthesized in our laboratory using *rac*-EtInd$_2$ZrCl$_2$/MAO (**2**/MAO) as catalyst. (The polymer characteristics are given in Table 3.) As expected, polyethene synthesized using **1**/MAO contains LCB, and so does poly(E-*co*-N) synthesized with the same catalyst. This is seen from the curvature of the plots at high molar masses. In addition, the presence of the voluminous norbornene units in the polymer chain significantly decreases the hydrodynamic volume of the macromolecules; i.e., [η] of poly(E-*co*-N) was much lower than [η] of polyethene of the same molar mass.

Table 3 summarizes the most important results of the molecular characterization and branching analysis of linear and branched polyethene and poly(E-*co*-N). Table 3 reports the weight-average molar mass M_w, [η], the polydispersity index M_w/M_n, and the branching parameters g' and LCB_{1000C}. We can see that g' and LCB_{1000C} values for the polyethene sample are typical for a branched polymer with a medium-high LCB frequency. On the basis of the g' and LCB_{1000C} results reported in Table 3, we can also state that a correlation between the degree of branching (number of LCBs) and the norbornene content in the copolymer exists: increasing $x_{N,copolymer}$ results in a decrease in the degree of branching, ($x_{N,copolymer}$ depends on $x_{N,feed}$, of course). Figure 8 shows a comparison of the MHS plot of branched polyethene and two branched poly(E-*co*-N) copolymers with different $x_{N,copolymer}$. When $x_{N,copolymer}$ increases, both [η] and the curvature of the plots decrease. The latter is in line with lower branching frequency with increasing $x_{N,copolymer}$, and the former is related to the lower hydrodynamic volume of poly(E-*co*-N) compared to polyethene, as shown in Figure 7.

The degree of branching in the poly(E-*co*-N) samples does not depend on the reaction time. Although the molar mass of the copolymer increases with time, as shown in Figures 3−6, the LCB_{1000C} value remains constant. This is illustrated in Figure 9 where the MHS plots of six poly(E-*co*-N) samples taken at different

Table 3. Summarized Results for Linear and Branched Polyethene and Poly(E-*co*-N)

polymer	catalyst	$x_{N,copolymer}$[a]	M_w (kg/mol)	M_w/M_n	$[\eta]$ (dL/g)	g' [b]	LCB_{1000C}[c]
polyethene	*d*	0.00	54.3	2.7	0.94	1.00	0.00
polyethene	**1**/MAO	0.00	349.3	4.8	1.82	0.62	1.54
poly(E-*co*-N)	**2**/MAO	0.40	182.5	1.4	0.85	1.00	0.00
poly(E-*co*-N)	**1**/MAO	0.26	534.0	2.0	1.84	0.64	0.87
poly(E-*co*-N)	**1**/MAO	0.44	533.5	1.8	1.85	0.66	0.83

[a] Norbornene molar fraction in the copolymer. [b] Branching index calculated using eqs 1a−c. [c] LCB per 1000C atom calculated using eqs 1−3. [d] NBS1475 standard.

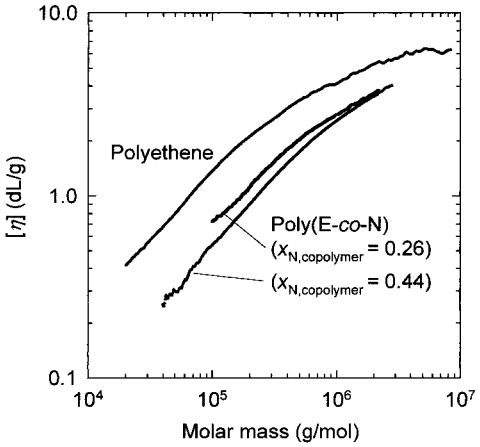

Figure 8. Comparison of the Mark−Houwink−Sakurada plot for branched polyethene and two long chain branched poly(E-*co*-N) samples with $x_{N,copolymer} = 0.26$ and $x_{N,copolymer} = 0.44$, respectively.

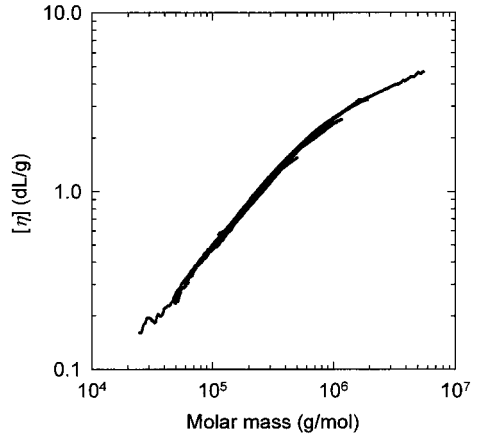

Figure 9. Comparison of the Mark−Houwink−Sakurada plot for long chained branched poly(E-*co*-N) sampled at different reaction times during the same run (reaction time = 10−60 min, M_w = 275−787 kg/mol, M_w/M_n = 1.5−2.0, $x_{N,copolymer}$ = 0.42, and norbornene conversion < 6.6%).

reaction times during the same run are reported. The six MHS plots are perfectly superimposed, and consequently, the degree of branching remained constant between 6 and 60 min reaction time. Furthermore, the data presented in Figure 9 show that the LCBs are evenly distributed in the copolymers.

It has been suggested that when **1**/MAO is used for polyethene synthesis, LCBs are formed by β-H transfer to the monomer followed by reinsertion of the macromonomer.[14,15] By analogy, the same mechanism can be assumed to account for LCB formation in poly(E-*co*-N) with the following important feature: β-H transfer occurs from E*-sites only. From N*-sites, β-H transfer to either the metal or any of the monomers is impossible.[9d] The very presence of LCB shows that the chain transfer by β-H transfer from E*-sites indeed occurs to some extent. However, when $x_{N,feed}$ is increased, LCB_{1000C} decreases, presumably because the chain transfer to Al from N*-sites becomes the main chain-transfer path. This interpretation is in line with the experimental observations; it is outlined in Scheme 2. Copolymers with both a high $x_{N,copolymer}$ and LCB_{1000C} cannot be synthesized with the chosen approach.

Table 4. Selected Characteristics of the Samples Characterized by Rheology and Reported in Figure 10

sample[a]	$x_{N,copolymer}$[b]	M_w (kg/mol)	M_w/M_n	$[\eta]$ (dL/g)	g' [c]	LCB_{1000C}[d]
a	0.00	349.3	4.8	1.82	0.62	1.54
b	0.42	262.6	2.2	0.95	0.74	0.52
c	0.46	95.1	2.2	0.39	1.00	0.00

[a] Catalyst: **1**/MAO. [b] Norbornene molar fraction in the copolymer. [c] Branching index calculated using eqs 1a−c. [d] LCB per 1000C atom calculated using eqs 1−3.

In Scheme 2, we summarize our proposed steps in the reaction scheme. The scheme is in line with the activity studies presented in Figures 1 and 2, assuming a slower propagation at N*-sites than that at E*-sites, the presence of LCB and its dependence of the $x_{N,feed}$, the uniform distribution of LCB, and a more quasi-living character with increasing $x_{N,feed}$. For a discussion of chain transfer, the main consideration is the ultimate unit (i.e., E*-, and N*-sites) since it alone allows for β-H transfer to occur. The reinsertion step during LCB formation, most probably, requires a second-order or, possibly, even a higher-order Markov model since the EE*-site is less sterically hindered than the NE*- or EN*-site, and the macromonomer can be expected to insert easier into the EE*-site. For steric reasons, we also expect that the macromonomer will reinsert easier if the unsaturated end group is next to an ethene unit. In other words, the branch point in the copolymer is expected to be in a locally ethene-rich part of the copolymer molecule.[39]

3.3. Rheology. Melts of poly(E-*co*-N) containing LCB are expected to show different flow properties, such as a higher zero-shear viscosity and shear thinning, compared to linear copolymers with otherwise similar characteristics. We characterized a selected set of our poly(E-*co*-N) samples by the rheological method. Selected characteristics of the samples are given in Table 4.

The van Gurp−Palmen plot given in Figure 10 is sensitive to the width of MMD and to molecular topology. Since M_W/M_n for the majority of samples chosen is ∼2, the effect of the molecular weight distribution can be neglected. Moving from high to low values of $|G^*|$, the van Gurp−Palmen (vGP) curve of a linear polymer, i.e., in the absence of LCB, drops, passes a minimum at $G_N°$, rises up, and passes an inflection point before it finally reaches the 90° plateau that indicates the terminal flow region.[42] Referring to Figure 10: The curve of $x_{N,copolymer} = 0.46$ (sample c) is typical for a "linear" polymer, without LCB, in agreement with SEC

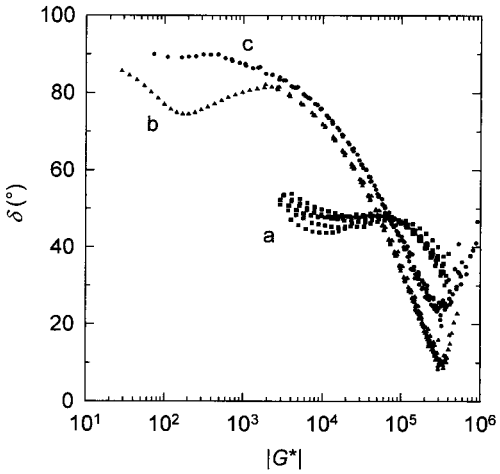

Figure 10. van Gurp−Palmen plot from rheology. The phase angle (δ) as a function of the absolute value of the dynamic shear modulus ($|G^*|$). Characteristics of the polymer samples a−c are given in Table 4.

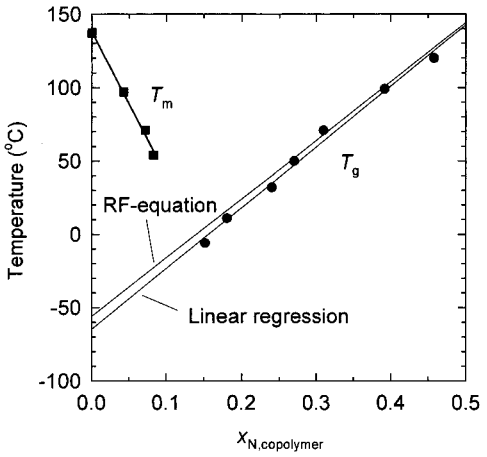

Figure 11. Glass transition temperature (T_g) and melting temperature (T_m) for poly(E-*co*-N) containing various molar fractions of norbornene ($x_{N,copolymer}$). For comparison, the empirical linear relation between T_g and $x_{N,copolymer}$ proposed by Ruchatz and Fink[9b] (RF equation) has been included.

data. In contrast, the vGP curve of polyethene ($x_{N,copolymer} = 0.0$) (sample a) clearly deviates from this curve, which features the onset of plateau at $|G^*|$ values below $G_N°$ and δ_c values around 45°, which is found characteristic for polymer mixtures of linear and LCB species of 1:1 composition.[43] In the norbornene-containing sample b, we can tell from the deviation to the curves of the linear pendant that the LCB is indeed present, but to a much lower degree than in the polyethene reference sample. $x_{N,copolymer} = 0.42$ (sample b) is essentially linear with few LCB molecules which can be concluded from the observation that a minimum is found at δ_c of 70−75° and at $|G^*|$ values of 4 decades below $G_N°$. A minimum in this region is found for polymer mixtures containing up to 5% long chain branched chains in a linear matrix. Apart from the detection of the long chain branches, it is interesting to note that the $G_N°$ minimum could be reached which is usually inaccessible for polyolefins since this region corresponds to low temperatures, according to the time−temperature superposition principle, at which crystallization normally occurs. This is another experimental proof that the bulky norbornene substituent inhibits crystallization and leads to amorphous polymers. In conclusion, SEC and rheology analysis agree on the linear or branched polymer architecture of the considered samples; the methodology based on SEC with on-line viscometry affords a reliable and quantitative analysis.

3.4. Thermal Properties. Increased T_g is an important characteristic of poly(E-*co*-N) compared to polyethene. Because of a higher number of chain ends and tertiary branch point carbons, LCB may be expected to influence the T_g of poly(E-*co*-N) obtained using **1**/MAO compared to T_g of linear copolymers. We measured the T_g of selected poly(E-*co*-N) samples that differed mainly in the amount of LCB and $x_{N,copolymer}$. The data are plotted in Figure 11. Copolymers with low norbornene fractions ($x_{N,copolymer} < 0.083$) showed a melting temperature (T_m) which decreased linearly with increasing $x_{N,copolymer}$. At higher $x_{N,copolymer}$, no melting transition was observable by DSC. In the interval $0.152 < x_{N,copolymer} < 0.458$, T_g increases with increasing $x_{N,copolymer}$ in a manner described by an empirical linear relation reported by Ruckhatz and Fink[9c] (RF equation). However, as the $x_{N,copolymer}$ is lowered, a small difference between the RF equation and our experimental data becomes apparent. If a linear trend for the experimentally obtained T_g data is extrapolated to $x_{N,copolymer} = 0$ (polyethene) and compared to the value calculated from the RF equation, then the T_g of poly(E-*co*-N) obtained with **1**/MAO is 14 °C lower than that calculated using the RF equation. This is in accordance with a lowering of T_g due to the presence of a higher number of chain ends in the copolymers containing LCB; recall that the LCB frequency increases as $x_{N,copolymer}$ decreases, as described earlier.

4. Conclusion

In the present work, we copolymerized ethene and norbornene in toluene using $Me_2Si(Me_4Cp)(N^tBu)TiCl_2$/MAO as catalyst and studied the reaction kinetics and copolymer properties. We have demonstrated that poly(ethene-*co*-norbornene) containing long chain branches can be obtained and that the branching frequency and the catalytic activity decrease with increasing the norbornene molar feed fraction, opposite to the amounts of norbornene incorporated in the copolymers. The long chain branches were detected with both size exclusion chromatography and rheology. The size exclusion chromatography data show that the branches are evenly distributed in the copolymer molecules. The low concentration of long chain branches did not significantly influence on the glass transition temperature of the copolymers when compared to the literature data for linear copolymers. When poly(ethene-*co*-norbornene) was analyzed by means of rheology, the $G_N°$ minimum could be reached, most probably because the bulky bicyclic norbornene units inhibit crystallization.

We further demonstrated that the molecular weight increased with reaction time, and chain-transfer reactions were found to occur when the copolymerizations were carried out at 30 or 50 °C and high norbornene molar feed fractions. Under such conditions, the copolymerization can be considered as quasi-living. The lowest polydispersity index obtained was $M_w/M_n = 1.3$ for the copolymers obtained after 10 min reaction at 50 °C and at $x_{N,feed} = 0.983$.

A reaction scheme taking propagation, formation of long chain branches, and chain transfer to Al into account was proposed in order to account for the

observed relationship between the reaction conditions and the polymer architecture.

5. Experimental Details

General. All chemicals were handled and stored using standard glovebox and Schlenk techniques. **1** was obtained from Boulder Scientific Co. and used as received, MAO was dried under vacuum and stored as a powder, and toluene was distilled over sodium under a nitrogen atmosphere. Norbornene was distilled over potassium under a nitrogen atmosphere and used as a stock solution in toluene. Ethene was passed over molecular sieves (4 Å) and BTS to remove oxygen and water.

Polymerization. To a thoroughly dried round-bottom flask (500 mL), toluene and norbornene stock solution were transferred to give the desired amounts of norbornene and a total liquid volume of 200 mL after addition of MAO and **1**. The stirring rate (1250 rpm) and ethene pressure (1.1 atm) were set and kept constant during the runs, and equilibration was allowed. Finally, MAO (7.2 mmol) and catalyst (3.6 μmol), both dissolved in small amounts of toluene, were injected (Al/Ti = 2000). In single-run experiments, polymerization was typically allowed for 1 h before the polymer was precipitated in an ethanol (2 L)/HCl (40 mL) mixture, stirred overnight, filtered, stirred with ethanol overnight, filtered, and dried at 70 °C under vacuum. In the kinetic studies, a given volume (8−20 mL) was sampled from the reaction flask and immediately precipitated in acidic ethanol (10-fold of the sample volume, composition as above). Further workup was performed as given above.

^{13}C NMR. The copolymers were dissolved in $C_2D_2Cl_4$ with HMDS as internal standard. The spectra were recorded on a Bruker AM-270 spectrometer operating at 67.89 MHz (^{13}C) in the PFT mode at 103 °C. Peak assignments and further experimental details were as reported earlier.[12]

Size Exclusion Chromatography. The molar mass distribution (MMD) and the branching analysis were performed on a high-temperature dual-detector size exclusion chromatography (SEC) system. The SEC system was a GPCV2000 from Waters (Milford, MA) that uses two on-line detectors: a differential viscometer (DV) and a differential refractometer (DRI) as concentration detector. The description of this SEC−DV system has been reported elsewhere.[44] The experimental conditions were as follows: *o*-dichlorobenzene + 0.05% 2,6-di-*tert*-butyl-4-methylphenol (BHT, antioxidant) as mobile phase, 0.8 mL/min as flow rate, and a column temperature of 145 °C. The column set was composed of three GMH_{XL}-HT columns from TosoHaas (Stuttgart, Germany).

The universal calibration was constructed from 18 narrow MMD polystyrene standards, with the molar mass ranging from 162 to 5.48 × 10^6 g/mol.

Rheology. The copolymers where extracted with *o*-dichlorobenzene to remove catalysts residues. SEC and NMR characterizations were performed on the sample before and after extraction, and no differences were observed. Thus, the samples analyzed by rheology are representative of the full distribution of copolymers synthesized and not artifacts of the extraction.

A 1 wt % stabilizer (Irganox 1010 Irgafos 168, 1:4) was added to the purified materials, and these mixture were compression molded to approximately 1 mm thick disks 25 mm in diameter. With these specimen, the rheological measurements were done in a 25 mm plate geometry in the stress-controlled Bohlin CVO120. The reference temperature was set to be 170 °C. Prior to the measurement, four time sweep tests at 170 °C for 10 min at 125, 12.5, 1.25, and 0.125 rad/s were recorded and served as reference. The frequency sweep tests were done within the regime of linear viscoelasticity at angular frequencies ranging from 0.125 to 125 rad/s at 200, 190, 180, ..., 140 °C. Four time sweep test with the same settings as above proved thermal stability of the samples during measurement. A creep test followed with sample b in order to determine the rheological behavior near the terminal flow region. The creep data were converted into $G^*(\omega)$ as described elsewhere.[43] By this method, the master curve could be extended toward lower frequencies.

DSC. DSC was performed using a Perkin-Elmer Pyris 1. The copolymer sample (3−6 mg) was first cooled to −80 °C and kept there for 1 min. Then the sample was heated to 200 °C (20 °C/min), cooled to −80 °C (20 °C/min), heated to 200 °C (20 °C/min), and finally cooled to −80 °C (20 °C/min). The sample was kept under a He flow (30 mL/min) during the whole run, and the thermal transition temperature, T_g or T_m, was taken from the second scan.

Acknowledgment. Financial support from EC TMR Project Network N°ERB FMRX CT97-0116 GLASSCYCLICS is gratefully acknowledged. K.T. is also grateful for financial support from the Norwegian Research Council (NFR). Boulder Scientific Co. is acknowledged for providing the CGC. We thank Mr. G. Zannoni, Mr. A. Giacometti Schieroni, and Dr. F. Bertini for their cooperation with the NMR, SEC, and DSC analyses, respectively.

Supporting Information Available: Experimental copolymerization data and determination of copolymerization parameters. This material is available free of charge via the Internet at http://pubs.acs.org.

References and Notes

(1) Kaminsky, W.; Bark, A.; Arndt, M. *Makromol. Chem., Macromol. Symp.* **1991**, *47*, 83−93.
(2) Cherdron, H.; Brekner, M.-J.; Osan, F. *Angew. Makromol. Chem.* **1994**, *223*, 121−133.
(3) Sinn, H.; Kaminsky, W. *Adv. Organomet. Chem.* **1980**, *18*, 99−149.
(4) Brintzinger, H.-H.; Fischer, D.; Mülhaupt, R.; Rieger, B.; Waymouth, R. M. *Angew. Chem., Int. Ed. Engl.* **1995**, *34*, 1143−1170.
(5) Britovsek, G. J. P.; Gibson, V. C.; Wass, D. F. *Angew. Chem., Int. Ed.* **1999**, *38*, 428−447.
(6) Ittel, S. D.; Johnson, L. K.; Brookhart, M. *Chem. Rev.* **2000**, *100*, 1169−1204. (b) Coates, G. W. *Chem. Rev.* **2000**, *100*, 1223−1252. (c) Resconi, L.; Cavallo, L.; Fait.; A.; Piemontesi, F. *Chem. Rev.* **2000**, *100*, 1253−1346.
(7) Shapiro, P. J.; Bunel, E.; Schaefer, W. P.; Bercaw, J. E. *Organometallics* **1990**, *9*, 867−869.
(8) Okuda, J. *Chem. Ber.* **1990**, *123*, 1649−1651.
(9) Ruchatz, D.; Fink, G. *Macromolecules* **1998**, *31*, 4669−4673. (b) Ruchatz, D.; Fink, G. *Macromolecules* **1998**, *31*, 4674−4680. (c) Ruchatz, D.; Fink, G. *Macromolecules* **1998**, *31*, 4681−4683. (d) Ruchatz, D.; Fink, G. *Macromolecules* **1998**, *31*, 4684−4686.
(10) McKnight, A. L.; Waymouth, R. M. *Chem. Rev.* **1998**, *98*, 2587−2598.
(11) McKnight, A. L.; Waymouth, R. M. *Macromolecules* **1999**, *32*, 2816−2825.
(12) Provasoli, A.; Ferro, D. R.; Tritto, I.; Boggioni, L. *Macromolecules* **1999**, *32*, 6697−6706. (b) Tritto, I.; Marestin, C.; Boggioni, L.; Zetta, L.; Provasoli, A.; Ferro, D. R. *Macromolecules* **2000**, *33*, 8931−8944. (c) Tritto, I.; Marestin, C.; Boggioni, L.; Sacchi, M. C.; Brintzinger, H.-H.; Ferro, D. R. *Macromolecules* **2001**, *34*, 5770−5777. (d) Tritto, I.; Boggioni, L.; Jansen, J. C.; Thorshaug, K.; Sacchi, M. C.; Ferro, D. R. *Macromolecules* **2002**, *35*, 616−623.
(13) Lai, S.-Y.; Wilson, J. R.; Knight, G. W.; Stevens, J. C. Dow Chemical Company, Elastic substantially linear olefin polymers, U.S Patent No. 5278272, 1994.
(14) Wang, W.-J.; Yan, D.; Zhu, S.; Hamielec, A. E. *Macromolecules* **1998**, *31*, 8677−8683.
(15) Woo, T. K.; Margl, P. M.; Ziegler, T.; Blöchl, P. E. *Organometallics* **1997**, *16*, 3454−3468.
(16) Walter, P.; Trinkle, S.; Suhm, J.; Mäder, D.; Friedrich, C.; Mülhaupt, R. *Macromol. Chem. Phys.* **2000**, *201*, 604−612.
(17) Jansen, J. C.; Mendichi, R.; Locatelli, P.; Tritto, I. *Macromol. Rapid Commun.* **2001**, *22*, 1394−1398.
(18) Malmberg, A.; Kokko, E.; Lehmus, P.; Löfgren, B.; Seppälä, J. V. *Macromolecules* **1998**, *31*, 8448−8454.
(19) Randall, J. C. *J. Macromol. Sci., Rev. Macromol. Chem. Phys.* **1989**, *C29*, 201−317.

(20) For example: (a) Vega, J. F.; Muñoz-Escalona, A.; Santamaría, A.; Muñoz, M. E.; Lafuente, P. *Macromolecules* **1996**, *29*, 960−965. (b) Carella, J. M. *Macromolecules* **1996**, *29*, 8280−8281.

(21) Wood-Adams, P. M.; Dealy, J. M. *Macromolecules* **2000**, *33*, 7481−7488.

(22) Foster, G. N.; MacRury, T. B.; Hamielec, A. E. In *Liquid Chromatography of Polymers and Related Materials*; Cazes, J., Delmare, X., Eds.; Chromat. Sci. Series; Marcel Dekker: New York, 1980; Vol. 13, pp 143−171.

(23) Lecacheux, D.; Lesec, J.; Quivoron, C. *J. Appl. Polym. Sci.* **1982**, *27*, 4867−4877.

(24) Mirabella, F. M.; Wild, L. In *Polymer Characterization*; Claver, C. D., Provder, T., Eds.; *Adv. Chem. Ser.* **1990**, *227*, 23−44.

(25) Zimm, B.; Stockmayer, W. H. *J. Chem. Phys.* **1949**, *17*, 1301−1314.

(26) By ^{13}C NMR, the molar fraction of norbornene in the copolymer was calculated as $x_{N,copolymer} = [2I(C_7) + I(C_1-C_2) + I(C_2-C_3)]/3I(CH_2)$, where $I(CH_2)$, $I(C_7)$, $I(C_1-C_2)$, and $I(C_2-C_3)$ are the peak areas in the ranges 26−30, 30−36, 34−42, and 43−54 ppm.

(27) Based on a large number of poly(E-*co*-N) samples synthesized using different metallocenes, we have established a linear calibration curve ($r^2 = 0.996$) between the SEC RI detector area per microgram of injected sample and the weight fraction of norbornene in the sample as determined by ^{13}C NMR. From this calibration curve, we estimated the norbornene fractions in the copolymers based on the data obtained from the SEC traces. Under our SEC conditions, the RI signal is negative below 48.65 wt % norbornene ($x_{N,copolymer} = 0.220$) in the copolymer and positive for copolymers containing more norbornene.

(28) The curve fitting was performed using SigmaPlot from Jandel Scientific (version 1.02). The experimental data were fitted to the copolymerization equations that relates the feed composition and the copolymer composition,[29] and we used the built-in minimization routine to find the reactivity ratios.

(29) Odian, G. *Principles of Polymerization*, 3rd ed.; Wiley: New York, 1991; pp 457−504.

(30) Copolymerization plots and equations are given as Supporting Information.

(31) Fischer, D.; Mülhaupt, R. *J. Organomet. Chem.* **1991**, *417*, C7−C11.

(32) Wester, T. S.; Johnsen, H.; Kittilsen, P.; Rytter, E. *Macromol. Chem. Phys.* **1998**, *199*, 1989−2004.

(33) Thorshaug, K.; Støvneng, J. A.; Rytter, E.; Ystenes, M. *Macromolecules* **1998**, *31*, 7149−7165.

(34) For ideal living polymerization M_n = yield/(number of active sites), since the number of macromolecules produced is equal to the number of active sites. Chain-transfer reactions are detected by lower values of the experimentally determined M_n compared to the theoretical ones; i.e., the number of macromolecules is higher than the number of active Ti centers.

(35) Kissin, Y. V. *Isospecific Polymerization of Olefins;* Springer-Verlag: New York, 1985. (b) Natta, G.; Pasquon, I. *Adv. Catal.* **1959**, *11*, 1−66.

(36) Busico, V.; Cipullo, R.; Esposito, V. *Macromol. Rapid Commun.* **1999**, *20*, 116−121.

(37) Jansen, J. C.; Mendichi, R.; Sacchi, M. C.; Tritto, I. Submitted for publication.

(38) Beck, S.; Lieber, S.; Schaper, F.; Geyer, A.; Brintzinger, H −H. *J. Am. Chem. Soc.* **2001**, *123*, 1483−1489.

(39) In principle, long chain branches in poly(E-*co*-N) could be analyzed by ^{13}C NMR. Microstructure analysis of poly(E-*co*-N) has received a great amount of attention during recent years,[9b,11,12,40,41] and it is now possible to quantitatively determine the microstructure of poly(E-*co*-N) at tetrad level within an accuracy of 1−2%.[12c] The proposed branched structure will influence the chemical shifts of the adjacent norbornene units as well as those of methylene and of methine carbons of a long chain branched polyethylene. It would be relatively easier to predict the chemical shifts of secondary and tertiary carbons of the ethylene part of the branching. However, depending on the distance of the norbornene unit from the tertiary carbon of the branch point, the chemical shifts of carbons of the three branches are expected to be different, and thus a scattering of the signals is expected. The level of branching found in the copolymers is below 1 LCB/1000 carbons. To experimentally prove the proposed branch structure, a detailed and nontrivial study of high-resolution ^{13}C NMR is required. Quantitative spectra recorded with sensitivity greater than 0.5/1000 are needed.

(40) Wendt, R. A.; Mynott, R.; Hauschild, K.; Ruchatz, D.; Fink, G. *Macromol. Chem. Phys.* **1999**, *200*, 1340−1350.

(41) Arndt-Rosenau, M.; Beulich, I. *Macromolecules* **1999**, *32*, 7335−7343.

(42) Trinkle, S.; Friedrich, C. *Rheol. Acta* **2001**, *40*, 322−328.

(43) Trinkle, S.; Walter, P.; Friedrich, C. *Rheol. Acta*, in press**.**

(44) Brun, Y.; Nielson, R.; Tacconi, R. *Proc. Int. GPC Symp. '98, Phoenix, AZ* **1998**, 415−436.

MA011949O